Wormholes in Vegh–dRGT massive gravity: a null-energy transparency theorem, horizon obstruction, and exact isotropic solutions

Sudan Hansraj[1†] Ayan Banerjee[1]

[1]Astrophysics Research Centre, School of Mathematics, Statistics and Computer Science, University of KwaZulu-Natal, Private Bag X54001, Durban 4000, South Africa

Abstract: We study static, spherically symmetric wormholes in de Rham–Gabadadze–Tolley massive gravity with the spatially degenerate Vegh reference metric. The effective fluid associated with the massive graviton does not contribute to the combination of density and radial pressure constrained by the flare-out condition; thus, it does not affect the null energy condition along radial light rays. This result holds for the entire degenerate class of reference metrics, for all four interaction potentials, and for any static, spherically symmetric geometry. The same property identifies the Vegh choice as the only consistent one. Consequently, the matter sector alone must violate the null energy condition at every throat, exactly as in general relativity. This corrects a claim repeatedly made in the massive-gravity wormhole literature.

We then determine the allowed locations of throats. Wormholes with isotropic pressure fall into two families. One lies beyond the cosmological horizon of the theory's own vacuum and has no static exterior; it is empty in general relativity and is generated by the graviton coupling. The other lies inside that horizon and requires a rapidly decreasing redshift function. We provide exact perfect-fluid solutions for both families. In the second family, the graviton term can convert the tension at the throat into ordinary pressure. A thin shell closes the configuration, and its surface stresses and exotic-matter content are obtained in closed form. The shells are radially unstable, and light rays near the throat follow an unstable circular orbit.

Keywords: Wormhole, Energy Conditions,, Vegh--dRGT massive gravity

DOI: 10.1088/1674-1137/aeb48f **CSTR:**

CPC Accepted

I. INTRODUCTION

A wormhole is a tunnel in spacetime. It links two regions through a narrow neck, called the throat, where the areal radius is smallest. The idea originated with the bridge solution of Einstein and Rosen [1] and the geometrodynamics of Misner and Wheeler [2]. Morris and Thorne [3] formulated it as a concrete problem. They asked what matter is needed to keep the throat open. Their answer is the flare-out condition, which comes at a cost: the null energy condition (NEC) must be violated at the throat. The same conclusion follows from the causality analysis of Morris, Thorne and Yurtsever [4] and from the cut-and-paste constructions of Visser [5]. This result is standard and is presented in the book of Visser [6], in the throat analysis of Hochberg and Visser [7], and in the review of Lobo [8]. Matter that violates the NEC is called exotic. No known laboratory fluid behaves in this way.

Because this violation cannot be eliminated, the next question is how much of it is required. Visser, Kar and Dadhich [9] addressed this question with a volume integral of $\rho + p_r$, which measures the total exotic content of a configuration. Nandi, Zhang and Kumar [10] later refined this measure. Both studies show that the exotic content can be made arbitrarily small. The wormhole is cut off close to the throat and glued to a normal exterior across a thin shell. This is the surgical method of Visser [11], developed further for thin shells in general dimensions by Dias and Lemos [12].

One line of work retains general relativity (GR) and considers unusual matter. Phantom energy, which has $p < -\rho$, violates the NEC by construction. Sushkov [13] and Lobo [14, 15] constructed wormholes from it. Chaplygin gas and its generalisations were used in the same way [16, 17], and González et al. [18] studied how such throats evolve. In all these models, the exotic burden remains in the matter sector.

A second line of work modifies the theory of gravity instead. The extra terms in the field equations are moved to the right-hand side and interpreted as an effective fluid. The aim is for this fluid, rather than the physical matter, to violate the NEC at the throat. The $f(R,T)$ theory of

Received 17 August 2026; Accepted 14 October 2026

† E-mail: hansrajs@ukzn.ac.za

©2026 Chinese Physical Society and the Institute of High Energy Physics of the Chinese Academy of Sciences and the Institute of Modern Physics of the Chinese Academy of Sciences and IOP Publishing Ltd. All rights, including for text and data mining, AI training, and similar technologies, are reserved.

Harko et al. [19] has been used in this way many times [20−30], and some of these papers report throats held open by matter that is not exotic [31, 32]. The junction conditions of the theory have been derived separately [33]. Rastall gravity has been used for the same purpose [34−37]. Every such claim rests on one point: the effective fluid must contribute to the sum $\rho + p_r$ at the throat. If it does not, the claim cannot hold, regardless of how the rest of the calculation is arranged. We settle this point for massive gravity.

Massive gravity gives the graviton a mass. The linear theory contains a ghost. The resolution was found by de Rham and Gabadadze [38] and completed by de Rham, Gabadadze and Tolley [39]. Hassan and Rosen [40] then proved that the theory is free of the ghost at full nonlinear order. The construction is reviewed in Refs. [41, 42]. The mass term is built from a fixed reference metric, which does not satisfy independent field equations. Its contribution can also be interpreted as an effective fluid. That fluid is often called dark-energy-like, and this description has been taken to imply that it violates the energy conditions and can therefore hold a throat open.

The reference metric must be chosen. We use the spatially degenerate choice of Vegh [43], in which the time and radial entries vanish and only the angular block remains. It was introduced in a holographic setting, where it relaxes momentum [44] and where the graviton mass arises from a lattice [45]. It is also the choice used in the black-hole solutions of Cai et al. [46] and in later work on their thermodynamics [47]. Compact objects have also been studied in dRGT gravity: relativistic stars [48], neutron stars [49], and white dwarfs [50]. The stellar-structure problem in this gauge is treated separately by the present authors. The wormhole problem is set here in the same canonical variables.

The wormhole literature in dRGT gravity is limited, but it is uniform in one respect. Tangphati et al. [51] studied traversable wormholes in $f(R)$ massive gravity with an exponential shape function specified by hand, so the imprint of the graviton on the geometry was never extracted. Kamma et al. [52] treated wormholes on a massive-graviton background in a short proceedings contribution. The fullest treatment is that of Dutta, Roy, Pullisseri and Chakraborty [53]. They built ultrastatic anisotropic wormholes in dRGT–$f(R,T)$ and in dRGT–Einstein gravity, using the parameterisation of Ghosh, Tannukij and Wongjun [47], in which the graviton sector carries the effective stresses

$$\rho^{(g)} = -\frac{2\tilde{\gamma} - \Lambda r}{8\pi r}, \quad p_r^{(g)} = +\frac{2\tilde{\gamma} - \Lambda r}{8\pi r}, \quad p_t^{(g)} = \frac{\tilde{\gamma} - \Lambda r}{8\pi r}. \quad (1)$$

Bhar [54] constructed two further wormhole families in the same theory. Kumar, Maurya and Kiroriwal [55] fixed the shape function from dark-matter density profiles, and Chaudhary, Maurya and Kumar [56] adopted the same approach using galactic rotation curves. Evolving wormholes were treated in Ref. [57], and Landry et al. [58] studied Morris–Thorne geometries in $F(T)$ teleparallel gravity with an added dRGT mass term. Across this body of work, the same conclusion recurs: the graviton stresses violate the energy conditions, so a wormhole in massive gravity is a natural outcome.

Two issues motivate the present paper. The first is a gap in the literature. No study has treated the spatially degenerate Vegh gauge. Its effective fluid is a constant shift $\alpha - 1 = m^2C^2c_2$ together with a linear term of coefficient $\gamma/2 = m^2c_1C/2$. This differs in structure from (1), and it is the sector treated here for the first time in the wormhole context. The second is an error in the prevailing interpretation. The stresses (1) directly satisfy $\rho^{(g)} + p_r^{(g)} = 0$, so the graviton sector adds nothing to the sum constrained by the flare-out condition. Yet Ref. [53] concludes that the massive gravitons supply the negative energy density that keeps the throat open, and reports ordinary matter with $\rho + p_r \geq 0$ near the throat of an Einstein–massive wormhole. We show below that both statements conflict with the flare-out identity, and that they do so within the effective-stress split displayed in Ref. [53] itself.

Our first result is that this is not an isolated error. The property $\rho^{(g)} + p_r^{(g)} = 0$ holds for the entire diagonal spatially degenerate class of reference metrics, for all four dRGT potentials, and for an arbitrary static spherically symmetric metric. It is already visible in (1). It forces the matter alone to carry the NEC violation at every throat. The transparency theorem therefore applies to each of the constructions listed above, and any reported relief of the matter sector must arise from the curvature or torsion terms, never from the mass term.

The plan and main results are as follows. Section II presents the field equations and the canonical variables, and translates the Morris–Thorne conditions into them: a throat is a simple zero of the spatial potential. Section III proves the transparency theorem and derives its corollaries. Section IV derives the throat-slope formula for isotropic pressure and establishes a dichotomy between super-horizon wormholes with non-decreasing redshift and sub-horizon wormholes with steeply decreasing redshift. The ultrastatic isotropic class, empty in GR, exists in Vegh–dRGT gravity only beyond the cosmological zero of its own vacuum, and the coupling bound quoted in Sec. IV pushes such throats beyond ~ 50 km. Sections V and VI exhibit exact perfect-fluid wormholes realising each branch; the latter possesses a universal throat density and a graviton-generated window of positive throat pressure. Section VII completes the sub-horizon configuration with a Darmois–Israel shell that joins it to the exact vacuum, and evaluates the surface stresses and the exotic budget in closed form. Section VIII develops a finite-radius light-propagation diagnostic for the static-patch completion,

CPC Accepted

and Section IX summarises and outlines the programme. All symbolic claims in this paper have been verified by computer algebra.

II. FIELD EQUATIONS, CANONICAL VARIABLES, AND THE THROAT

We consider the four-dimensional dRGT action with couplings c_1, c_2 and the degenerate Vegh reference metric $f_{ab} = \mathrm{diag}(0, 0, C^2, C^2 \sin^2\theta)$, where C has dimensions of length [43, 46]. For the static, spherically symmetric line element

$$ds^2 = -e^{2\nu(r)}dt^2 + e^{2\lambda(r)}dr^2 + r^2 d\Omega^2, \tag{2}$$

The field equations for an anisotropic fluid are given by

$$\kappa r^2 \rho = e^{-2\lambda}(2r\lambda' - 1) + \alpha + \gamma r, \tag{3}$$

$$\kappa r^2 p_r = e^{-2\lambda}(2r\nu' + 1) - \alpha - \gamma r, \tag{4}$$

$$\kappa r^2 p_t = e^{-2\lambda}\left(r\nu' + r^2\nu'^2 - r\lambda' - r^2\lambda'\nu' + r^2\nu''\right) - \frac{1}{2}\gamma r, \tag{5}$$

where $\alpha = 1 + m^2 C^2 c_2$ and $\gamma = m^2 c_1 C$, and the unique static vacuum solution is $e^{-2\lambda} = e^{2\nu} = \alpha + \frac{1}{2}\gamma r - 2M/r$. In the canonical variables

$$x = Kr^2, \qquad e^{-2\lambda} = Z(x), \qquad e^{2\nu} = y^2(x), \tag{6}$$

The condition for isotropic pressure, $p_r = p_t = p$, is the master equation.

$$4x^2 Z\ddot{y} + 2x^2 \dot{Z}\dot{y} + \left(\dot{Z}x - Z + \alpha + \beta\sqrt{x}\right)y = 0, \tag{7}$$

where $\beta = \gamma/(2\sqrt{K})$, and the density and pressure are

$$\frac{\kappa\rho}{K} = -2\dot{Z} - \frac{Z-\alpha}{x} + \frac{2\beta}{\sqrt{x}}, \qquad \frac{\kappa p}{K} = \frac{4Z\dot{y}}{y} + \frac{Z-\alpha}{x} - \frac{2\beta}{\sqrt{x}}. \tag{8}$$

Given a prescribed seed $y(x)$, (7) is linear and first order in Z,

$$(2x^2\dot{y} + xy)\dot{Z} + (4x^2\ddot{y} - y)Z + (\alpha + \beta\sqrt{x})y = 0, \tag{9}$$

so that every tractable seed generates an exact solution by quadrature.

The Morris–Thorne form $ds^2 = -e^{2\Phi}dt^2 + (1 - b/r)^{-1}dr^2 + r^2 d\Omega^2$ corresponds to $Z = 1 - b/r$ and $y = e^{\Phi}$. A throat $b(r_0) = r_0$, together with the flare-out condition $b'(r_0) < 1$ and the absence of a horizon, translates into three statements about the canonical potentials: $Z(x_0) = 0$ is a *simple zero* approached from a region with $Z > 0$; its slope is positive, $\dot{Z}(x_0) > 0$, since $Z'(r) = (b - rb')/r^2 = (1 - b')/r_0$ at the throat; and $y(x_0)$ is finite and nonzero. The proper radial distance $\int dr/\sqrt{Z}$ converges across a simple zero, the areal radius is minimized there, and the geometry extends across the throat in the usual way. Thus, the center of the stellar problem is replaced by a zero of Z as the distinguished locus, and the same canonical apparatus applies.

A. The two potentials and the geometry of their zeros

Two metric functions enter the construction below and must be kept distinct. The first is the interior spatial potential $Z(x) = e^{-2\lambda}$, which, together with the independent redshift function $y^2(x) = e^{2\nu}$, governs the matter-filled region containing the throat. These two functions are related only through the master equation (7). The second is the vacuum potential

$$Z_{\mathrm{vac}}(x) = \alpha + \beta\sqrt{x} - \frac{2M\sqrt{K}}{\sqrt{x}}, \tag{10}$$

the unique static exterior solution of the theory, which contains no matter and in which the two potentials coincide, $e^{2\nu} = e^{-2\lambda} = Z_{\mathrm{vac}}$. It is of Schwarzschild–de Sitter type, with α replacing unity and with a graviton term that is linear, rather than quadratic, in the areal radius. The functions Z and Z_{vac} are never simultaneously active: on the interior interval, the geometry is described by Z; on the exterior interval, it is described by Z_{vac}. The two are related only by the Darmois–Israel conditions imposed at a single matching radius, x_b, which fix the shell stresses and the mass M. They do not coincide even there—the shell exists precisely because Z, Z_{vac}, and their slopes differ at x_b.

This distinction determines the character of the zeros, and three geometrically distinct situations arise. A simple zero of Z approached from $Z > 0$ with $\dot{Z}(x_0) > 0$ is a *throat*: the proper radial distance $\int dx/(2\sqrt{Kx}\sqrt{Z})$ remains finite across it, the areal radius is minimal, and the geometry flares outward. It is never a horizon because the zero occurs in the *spatial* potential; thus, $g_{rr} = 1/Z$ diverges, whereas $g_{tt} = -y^2$ remains finite and nonzero. A simple zero of Z with $\dot{Z} < 0$ is the opposite object: it is a sphere of *maximal* area at which the static Lorentzian region terminates, with Z becoming negative beyond it. It is not a throat, even though the condition $b(r_0) = r_0$ is satisfied there. By contrast, a zero of Z_{vac} is always a Killing

CPC Accepted

horizon because the static vacuum has $g_{tt} = -Z_{\rm vac}$; thus, the vanishing of the potential is the vanishing of g_{tt}, and ∂_t becomes null. The outer such zero, $x_c = Kr_c^2$, fixed by $\alpha^2 \geq 4|\gamma|M$ as in (23) below, is the cosmological horizon of the theory's own vacuum and the outer boundary of its static patch, entirely analogous to the horizon of the de Sitter static patch. The matching radius x_b is a zero of *neither* function; it is a free parameter of the construction. The physical content of the model therefore requires only that the window

$$x_0 < x_b < x_c \tag{11}$$

be non-empty—equivalently, that the throat lie within the static patch of its own vacuum. Whether this can be achieved is determined by the field equations; this is the subject of the dichotomy in Sec. IV.

III. RADIAL NULL-ENERGY TRANSPARENCY OF THE GRAVITON SECTOR

Consider a general diagonal, spatially degenerate reference metric

$$f_{ab} = \mathrm{diag}\big(0, 0, F(r), F(r)\sin^2\theta\big), \qquad F(r) > 0, \tag{12}$$

of which the Vegh gauge corresponds to the constant profile $F = C^2$, inserted into the *arbitrary* static metric (2); no field equations are used. The matrix $K^a{}_b = \sqrt{g^{ac}f_{cb}}$ is diagonal and has exactly two equal nonvanishing eigenvalues, $k = \sqrt{F}/r$. Throughout, we take the principal square root of the positive semidefinite matrix $g^{ac}f_{cb}$, which identifies the physical diagonal branch. For two equal eigenvalues, one finds $\mathcal{U}_3 = \mathcal{U}_4 = 0$ identically. The couplings c_3 and c_4 therefore drop out of the interaction tensor altogether, and a direct computation retaining all four potentials gives

$$\chi^t{}_t = \chi^r{}_r = -\frac{c_1\sqrt{F}}{r} - \frac{c_2 F}{r^2}, \qquad \chi^\theta{}_\theta = -\frac{c_1\sqrt{F}}{2r}, \tag{13}$$

This identity has been verified symbolically for arbitrary $F(r)$, $\Phi(r)$ and $b(r)$, demonstrating that it is an algebraic property of the entire class (12) for arbitrary couplings.

The generalisation is, however, constrained by consistency. With a fixed non-dynamical reference metric, the contracted Bianchi identity and matter conservation impose $\nabla_a\chi^a{}_b = 0$ on shell. Transparency further sharpens this condition: in the divergence $\nabla_a\chi^a{}_r = \partial_r\chi^r{}_r + \nu'(\chi^r{}_r - \chi^t{}_t) + (2/r)(\chi^r{}_r - \chi^\theta{}_\theta)$, the metric enters only through ν'. The coefficient of this term vanishes by (13), so the consistency condition is *metric-independent* and constrains only the fiducial profile:

$$\nabla_a\chi^a{}_r = -\frac{\big(c_1 r + 2c_2\sqrt{F}\big)F'(r)}{2r^2\sqrt{F}} = 0, \tag{14}$$

verified symbolically, with the t and angular components vanishing identically. For a smooth positive profile $F(r)$ and a nontrivial interaction sector $(c_1, c_2) \neq (0,0)$, equation (14) admits two branches: the constant profile $F = C^2$, which corresponds to the Vegh gauge, and the fine-tuned branch $\sqrt{F} = -c_1 r/(2c_2)$ (requiring $c_1 c_2 < 0$), for which $k = -c_1/(2c_2)$ is constant and the interaction tensor reduces to $\chi^a{}_b = \big[c_1^2/(4c_2)\big]\delta^a{}_b$ — a pure effective cosmological constant with no independent graviton contribution. Within the diagonal degenerate class, therefore, the Vegh profile is not merely a convenient choice but the *unique* consistent fiducial profile with nontrivial graviton stresses, and all consistent members of the class are radially transparent. Sectors such as those in Refs. [47, 53], whose effective stresses arise from genuine Stückelberg dynamics rather than from a fixed diagonal fiducial, restore conservation through the scalar equations of motion; for these sectors, transparency is confirmed by direct inspection of the stresses in (1), which manifestly satisfy $\rho^{(g)} + p_r^{(g)} = 0$. For the remainder of the paper, we work in the Vegh gauge, $F = C^2$, with C having dimensions of length. Writing the graviton contribution as an effective fluid, $\kappa\rho^{(g)} = m^2\chi^t{}_t$ and $\kappa p_r^{(g)} = -m^2\chi^r{}_r$ up to the sign conventions of (3)–(4), the first equality in (13) is the statement

$$\rho^{(g)} + p_r^{(g)} = 0 \qquad \text{pointwise, for any static metric.} \tag{15}$$

We refer to (15) as *radial null-energy transparency*: along radial null rays, the graviton sector is invisible to the Raychaudhuri focusing encoded by the flare-out condition. By the classification above, this property is shared by every consistent member of the diagonal degenerate class, and it also holds directly in the Stückelberg-based sector (1): no choice of couplings $c_1, \ldots, c_4$ or angular profile can evade it.

The corollary is immediate and precise. Adding (3) and (4) for the Morris–Thorne metric cancels the graviton terms and yields, at a throat where $b(r_0) = r_0$ and Φ is finite,

$$\kappa\big(\rho + p_r\big)\Big|_{r_0} = \frac{b'(r_0) - 1}{r_0^2} < 0, \tag{16}$$

with no dependence on m, c_1, c_2, or C. The matter sector alone must violate the radial NEC at the throat of every Morris–Thorne wormhole in Vegh–dRGT massive gravity, as in GR. The graviton sector can neither provide this

CPC Accepted

violation nor be arranged to evade it. In particular, under the effective-stress decomposition presented in Ref. [53], whose stresses (1) satisfy (15) manifestly, the claim in the Einstein–massive case that ordinary matter can satisfy the radial null energy condition at the throat while the gravitons supply the required negative energy is incompatible with the flare-out identity (16). In the $f(R,T)$-massive and $F(T)$-massive constructions [53, 58], any genuine alleviation of the requirement on the matter sector must originate from the curvature or torsion terms, never from the mass term.

This conclusion can be tested quantitatively against the published numerical calculations. This is important because Fig. 5 of Ref. [53] appears to show throats at which the null energy condition is satisfied. We adopt, for this paragraph, the notation of that work, writing $\alpha_{\rm f},\beta_{\rm f}$ for its $f(R,T)$ coefficients and γ,Λ for its graviton parameters, which differ from those of (3)–(5). For the linear choice $f=\alpha_{\rm f}R+\beta_{\rm f}T$, for which f_R is constant, the matter density and radial pressure are its Eqs. (29) and (30), and their sum is

$$\rho+p_r=\frac{\alpha_{\rm f}\left(rb'-b\right)}{r^3\left(8\pi+\beta_{\rm f}\right)}, \tag{17}$$

The graviton terms in γ and Λ cancel identically; this cancellation is already evident in the equations of Ref. [53]. Since flare-out requires $b-rb'>0$ at r_0, the right-hand side of (17) is negative at any genuine throat, for all values of the graviton parameters. The resolution of the apparent conflict therefore lies in the shape function. Differentiating Eq. (36) of Ref. [53] at the throat, for the parameters used in its Fig. 5 ($\alpha_{\rm f}=1$, $\beta_{\rm f}=2$, $\sigma=-1$), gives the closed form

$$b'(r_0)=-1+\frac{4(4\pi+1)}{4\pi+2}r_0\left(\Lambda r_0-2\gamma\right), \tag{18}$$

Thus, the flare-out condition at $r_0=1$ requires $\Lambda-2\gamma<(4\pi+2)/[2(4\pi+1)]\simeq 0.537$. Evaluating (18) for the four parameter sets shown in that figure, each at $r_0=1$, yields

$$b'(r_0)=\begin{cases}+1.533, & \gamma=0.01,\ \Lambda=0.7,\\ +1.682, & \gamma=-0.01,\ \Lambda=0.7,\\ -3.682, & \gamma=0.01,\ \Lambda=-0.7,\\ -1.004, & \gamma=0.001,\ \Lambda=0.001.\end{cases} \tag{19}$$

The first two values exceed unity. In these cases, the flare-out condition fails at $r=r_0$, where $Z=1-b/r$ has a simple zero with a *negative* slope. According to the classification in Sec. II A, this surface is a maximal-area sphere that terminates the static region, rather than a throat, and the assumed domain $r>r_0$ is not a static Lorentzian region. These are precisely the two cases for which Table I of Ref. [53] reports $\rho+p_r\geq 0$ from $r\simeq 0.87$ and $r\simeq 0.83$ outward. The remaining two parameter sets satisfy the flare-out condition, and for both, the same table records $\rho+p_r<0$ at $r_0=1$ — negative everywhere in one case and out to $r\simeq 6.09$ in the other. With this understanding, the published figure is not a counterexample to transparency, but rather an illustration of it. Every configuration in it that flares out violates the radial null energy condition at its throat, whereas every configuration that does not violate it is not a wormhole. The mechanism is also recognizably that of Sec. IV. An ultrastatic redshift, together with a sufficiently large positive effective cosmological term, turns the surface $b(r_0)=r_0$ from a minimal sphere into a maximal sphere. The dichotomy established below is the isotropic form of that statement, and (18) is its anisotropic counterpart in the variables of Ref. [53].

Transparency is radial rather than total. With the sign conventions of (3)–(5), $\kappa\rho^{(g)}=(1-\alpha)/r^2-\gamma/r$ and $\kappa p_l^{(g)}=\gamma/(2r)$, so the tangential combination is

$$\rho^{(g)}+p_l^{(g)}=\frac{1}{\kappa}\left(\frac{1-\alpha}{r^2}-\frac{\gamma}{2r}\right), \tag{20}$$

which is non-negative for the physical sign $\gamma<0$ (assuming $\alpha\leq 1$). Thus, the graviton sector violates neither the radial nor, for these signs, the tangential null energy condition. Nevertheless, it contributes fully to the tangential stress balance, reshapes the geometry away from the throat, and thereby constrains both the possible locations of throats and the distribution of exotic matter. The remainder of this paper quantifies these effects.

IV. THE THROAT-SLOPE FORMULA AND A HORIZON DICHOTOMY

For isotropic pressure, the master equation fully determines the system, and evaluating (9) at a throat $Z(x_0)=0$ yields the slope in closed form,

$$\dot{Z}(x_0)\;=\;-\frac{\left(\alpha+\beta\sqrt{x_0}\right)y(x_0)}{x_0\left[2x_0\dot{y}(x_0)+y(x_0)\right]}. \tag{21}$$

Equation (21) provides the isotropic wormhole existence test: a seed $y(x)$ admits a throat at x_0 if and only if the right-hand side is positive at that point.

First, consider any redshift function that is nondecreasing at the throat, $\dot{y}(x_0)\geq 0$ with $y>0$, including the ultrastatic class $y=\text{const}$ with zero tidal force. The denominator of (21) is then positive, and flare-out requires

CPC Accepted

$$\alpha+\beta\sqrt{x_0} < 0 \iff r_0 > \frac{2\alpha}{|\gamma|} \quad (\gamma<0). \tag{22}$$

In GR ($\alpha=1$, $\beta=0$), the left inequality is unsatisfiable: the ultrastatic isotropic class is empty and, more generally, no isotropic wormhole with a non-decreasing redshift exists. In Vegh–dRGT gravity, this class exists, enabled by the graviton coupling, but only for $\gamma<0$. However, (22) has an important consequence. For $\alpha>0$ and $\gamma=-|\gamma|<0$, the zeros of the vacuum function $Z_{\rm vac}=\alpha+\frac{1}{2}\gamma r-2M/r$ are obtained from $-\frac{1}{2}|\gamma|r^2+\alpha r-2M=0$, giving

$$r_\pm=\frac{\alpha\pm\sqrt{\alpha^2-4|\gamma|M}}{|\gamma|}, \tag{23}$$

which are real only for $0\le M\le\alpha^2/(4|\gamma|)$. Two cases arise. For $0\le M\le\alpha^2/(4|\gamma|)$, the vacuum has a static patch bounded by the outer zero $r_c\equiv r_+\le 2\alpha/|\gamma|$, while (22) places the throat beyond it, $r_0>2\alpha/|\gamma|\ge r_c$. For $M>\alpha^2/(4|\gamma|)$, the discriminant is negative, and the vacuum has no static region. In either case, the non-decreasing-redshift branch admits no static-vacuum completion. Thus, such a wormhole cannot be joined to any static region of its own vacuum; it is a super-horizon structure. We therefore obtain a dichotomy for isotropic wormholes in this theory: either the redshift function is non-decreasing at the throat, and the wormhole exists only beyond the cosmological zero of the vacuum, with no static exterior completion; or the wormhole is sub-horizon, in which case (21) forces

$$2x_0\,\dot{y}(x_0)+y(x_0) < 0, \tag{24}$$

equivalently, $\left[d\ln y/d\ln x\right]_{x_0}<-\frac{1}{2}$, meaning that the redshift function falls faster than $x^{-1/2}$ at the throat.

We emphasize the logical order: the horizon obstruction itself—a purely geometric consequence of the slope formula—excludes any static-vacuum completion of the nondecreasing-redshift branch. The compact-star analysis of this theory bounds the coupling as $|\gamma_1|=|m^2c_1C|\lesssim 4\times10^{-2}\,\mathrm{km}^{-1}$, so for $\alpha\approx1$ the excluded branch is additionally restricted to $r_0\gtrsim 50\,\mathrm{km}$. Static isotropic wormhole candidates that admit a static Vegh-vacuum exterior must therefore belong to the steep-redshift branch (24). We now exhibit exact solutions that realize each branch.

V. THE ULTRASTATIC WORMHOLE: AN EXACT SUPER-HORIZON SOLUTION

The ultrastatic condition $y=\text{const}$ eliminates the derivative terms in (7), which then requires precisely the reduction whose general solution is

$$Z(x)=\alpha+2\beta\sqrt{x}+K_2\,x. \tag{25}$$

The stellar interpretation requires $Z>0$ on a shell, whereas the wormhole interpretation selects the complementary regime $\beta^2>\alpha K_2$, $\beta<0$, $K_2>0$, in which Z has two positive zeros, $\sqrt{x_\pm}=\left[|\beta|\pm\sqrt{\beta^2-\alpha K_2}\right]/K_2$. Writing $u_\pm=\sqrt{x_\pm}$ and $D=\beta^2-\alpha K_2>0$, the slopes at the two zeros can be written in the compact form

$$\dot{Z}(x_+)=+\frac{\sqrt{D}}{u_+}>0, \qquad \dot{Z}(x_-)=-\frac{\sqrt{D}}{u_-}<0, \tag{26}$$

Thus, the outer zero is a throat, with the flare-out condition equivalent to $|\beta|\sqrt{x_+}>\alpha$, reproducing (22). The inner zero is *not* a horizon — $g_{tt}=-1$ remains finite and nonzero there—but a maximal-area two-sphere bounding the disjoint Lorentzian branch $x\le x_-$. The interval between the roots has $Z<0$ and is excluded, and the wormhole occupies $x\ge x_+$. The matter is a genuine perfect fluid with

$$\frac{\kappa\rho}{K}=-3K_2-\frac{2\beta}{\sqrt{x}}, \qquad \frac{\kappa p}{K}=K_2=\text{const}, \tag{27}$$

Thus, the pressure is uniform and positive, whereas the density is negative throughout the wormhole domain — the fluid is exotic through its density, and $\rho+p<0$ everywhere, consistent with the transparency theorem. The representative case $\alpha=1$, $\beta=-3/2$, $K_2=2$, with a throat at $x_0=1$, $\dot{Z}(x_0)=1/2$, $\kappa\rho/K=-3$, and $\kappa p/K=2$, is shown in Figs. 1–3. Asymptotically, $\kappa\rho/K\to-3K_2$ and $\kappa p/K=K_2$, corresponding to an equation of state $w=-1/3$: the wormhole is supported at large distances by a curvature-like halo, and the geometry is not asymptotically flat — as it cannot be, since by the dichotomy this solution lies beyond the cosmological zero of the vacuum and admits no static vacuum completion. It provides an explicit and, to our knowledge, first exact demonstration that the ultrastatic isotropic class, empty in GR, is populated in massive gravity, while simultaneously illustrating why that population is incompatible with a static astrophysical exterior.

VI. A SUB-HORIZON EXACT FAMILY FROM A STEEP SEED

The steep-redshift branch (24) is most simply realized by the seed

CPC Accepted

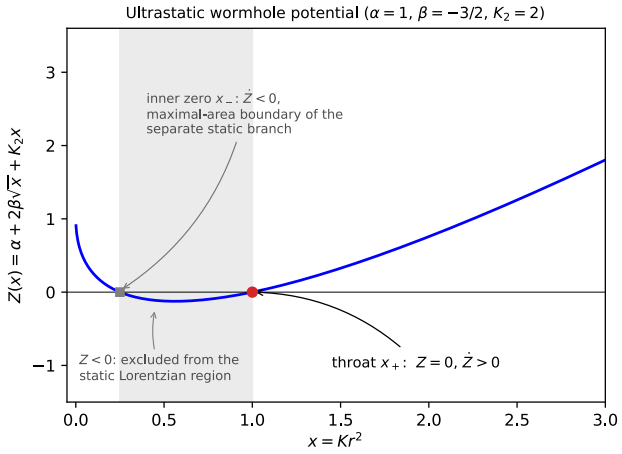


Fig. 1. (color online) The ultrastatic potential (25) for $\alpha = 1$, $\beta = -3/2$, and $K_2 = 2$. The outer zero is the throat. The inner zero, where $\dot{Z} < 0$, is the maximal-area boundary of the separate static branch $x \le x_-$ and plays no role in the wormhole domain $x \ge x_+$. The shaded interval has $Z < 0$ and is therefore excluded from the static Lorentzian region.

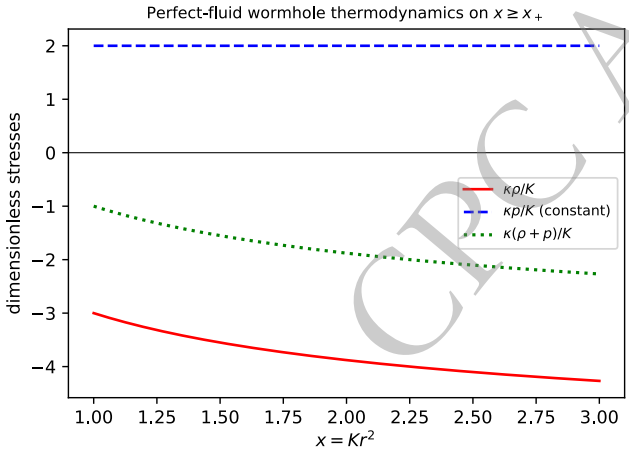


Fig. 2. (color online) Density, uniform pressure, and radial NEC combination for the ultrastatic wormhole on $x \ge x_0$. The violation $\rho + p < 0$ is carried entirely by the matter sector, as required by the transparency theorem.

$$y(x) = \frac{1}{x}, \qquad e^{2\nu} \propto \frac{1}{x^2}, \tag{28}$$

for which $2x\dot{y} + y = -1/x < 0$ everywhere. Substituting (28) into (9) yields the linear equation $x\dot{Z} - 7Z = \alpha + \beta\sqrt{x}$, whose general solution is

$$Z(x) = c_7 x^7 - \frac{\alpha}{7} - \frac{2\beta}{13}\sqrt{x}, \tag{29}$$

This expression was verified symbolically against the master equation. The integration constant controls the throat: imposing $Z(x_0) = 0$ fixes $c_7 = \left[\alpha/7 + (2\beta/13)\sqrt{x_0}\right]/x_0^7$ and yields the notably compact throat

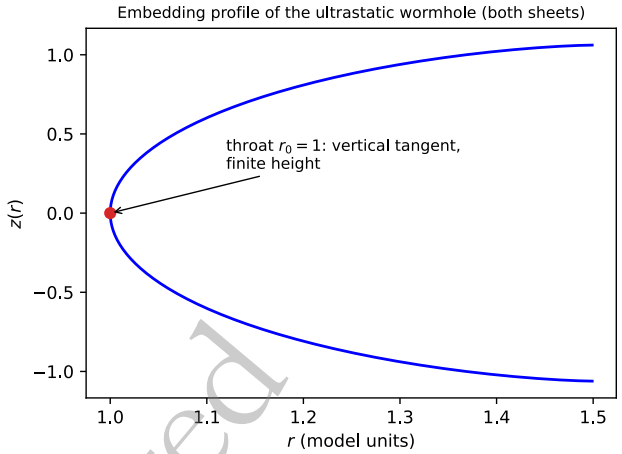


Fig. 3. (color online) Embedding profile of the representative ultrastatic wormhole (both sheets) in the region $Z < 1$.

data

$$\dot{Z}(x_0) = \frac{\alpha + \beta\sqrt{x_0}}{x_0}, \qquad \left.\frac{\kappa\rho}{K}\right|_{x_0} = -\frac{\alpha}{x_0},$$
$$\left.\frac{\kappa p}{K}\right|_{x_0} = \frac{2|\beta|\sqrt{x_0} - \alpha}{x_0}. \tag{30}$$

Three features deserve emphasis. First, the flare-out condition now requires $\alpha + \beta\sqrt{x_0} > 0$, i.e. $\sqrt{x_0} < \alpha/|\beta|$: the throat lies *inside* the cosmological radius, making this family the astrophysically relevant branch of the dichotomy. Second, the throat density has the notably simple value $\rho(x_0) = -\alpha K/(\kappa x_0)$ and contains no dependence on the graviton coupling β; as the seed tower below makes explicit through (34), this value is specific to the $s = 1$ family. This contrasts with the throat pressure discussed in the third point, which is seed-independent at every isotropic throat. The matter is therefore unavoidably exotic at the throat, as the theorem requires. Third, the throat *pressure* changes sign at $\sqrt{x_0} = \alpha/(2|\beta|)$: on the graviton-generated window

$$\frac{\alpha}{2|\beta|} < \sqrt{x_0} < \frac{\alpha}{|\beta|}, \tag{31}$$

The throat is supported by exotic density with *positive* pressure, whereas in the GR limit $\beta \to 0$ the window closes, and the throat can be supported only by tension, $p(x_0) = -\alpha K/(\kappa x_0) < 0$. The graviton term thus converts throat tension into ordinary pressure—a distinct qualitative effect of the massive sector, complementary to the transparency theorem. Figures 5 and 6 show the representative case $\alpha = 1$, $\beta = -3/2$, $\sqrt{x_0} = 1/2$, which lies well within the window (31): the throat is inside the static patch of the vacuum, and a finite junction window separates it from the cosmological zero.

CPC Accepted

In fact, the throat pressure in (30) applies much more generally than to the seed solution from which it was derived. Evaluating the second of (8) on any throat eliminates the $\dot{y}/y$ term together with Z, so that

$$\left.\frac{\kappa p}{K}\right|_{x_0} = \frac{2|\beta|\sqrt{x_0}-\alpha}{x_0} \qquad \text{for } \textit{every} \text{ isotropic wormhole,} \tag{32}$$

independent of the redshift profile: the positive-throat-pressure window (31) is universal, and its lower edge, $\sqrt{x_0}=\alpha/(2|\beta|)$, is a seed-independent feature of the theory. The seed dependence resides entirely in the slope and, consequently, in the throat density. Indeed, the single seed (28) generalises to the tower $y=x^{-s}$ with $s>1/2$, for which (9) integrates to

$$Z_s(x) = c\,x^{\frac{4s^2+4s-1}{2s-1}} - \frac{\alpha}{4s^2+4s-1} - \frac{2\beta\sqrt{x}}{8s^2+6s-1}, \tag{33}$$

verified symbolically for arbitrary s, with the throat slope $\dot{Z}(x_0)=(\alpha+\beta\sqrt{x_0})/[(2s-1)x_0]$—corresponding to sub-horizon flare-out throughout the tower —and the throat density

$$\left.\frac{\kappa\rho}{K}\right|_{x_0} = \frac{\alpha(2s-3)-4|\beta|\sqrt{x_0}\,(s-1)}{(2s-1)\,x_0}. \tag{34}$$

With $w\equiv|\beta|\sqrt{x_0}/\alpha\in(0,1)$, the expression in equation (34) is positive below the curve $w=(2s-3)/[4(s-1)]$, which exists for $s>3/2$ and approaches the universal pressure threshold $w=1/2$ as $s\to\infty$. Thus, the (s,w) plane is partitioned into the phase diagram shown in Fig. 4: throats with positive pressure and negative density ($w>1/2$), throats with positive density supported by tension ($s>3/2$ and small w), and a wedge in which both quantities are negative. Positive density and positive pressure never coexist at a throat—an immediate consequence of the transparency identity, since $\rho+p=-2\dot{Z}(x_0)K/\kappa<0$ there. Therefore, the diagram exhausts the possibilities, and steep seeds redistribute throat exoticity between the density and pressure channels in a fully explicit way.

A. Role of the seed

Because the redshift function is the free input in this scheme, it is useful to state precisely which of the preceding conclusions can be altered by changing the seed. Three cannot be altered. The transparency identity (15) was established for an arbitrary static spherically symmetric metric, without imposing any field equations, and therefore holds for every seed. Its corollary (16) is likewise an identity at any throat: whichever y is chosen, the matter violates the radial null energy condition there, and the magnitude of the violation is fixed by $b'(r_0)$ alone.

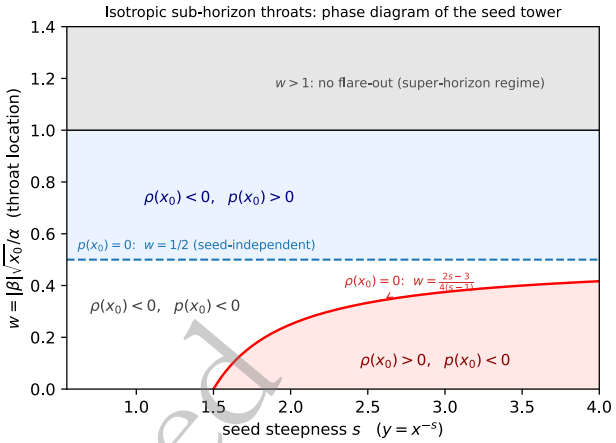


Fig. 4. (color online) Phase diagram of isotropic subhorizon throats for the seed tower $y=x^{-s}$ in the plane defined by the steepness s and throat location $w=|\beta|\sqrt{x_0}/\alpha$. The flare-out condition requires $w<1$; the throat pressure changes sign along the universal, seed-independent line $w=1/2$; and the throat density changes sign along $w=(2s-3)/[4(s-1)]$. Positive density and positive pressure never coexist, as required by radial transparency.

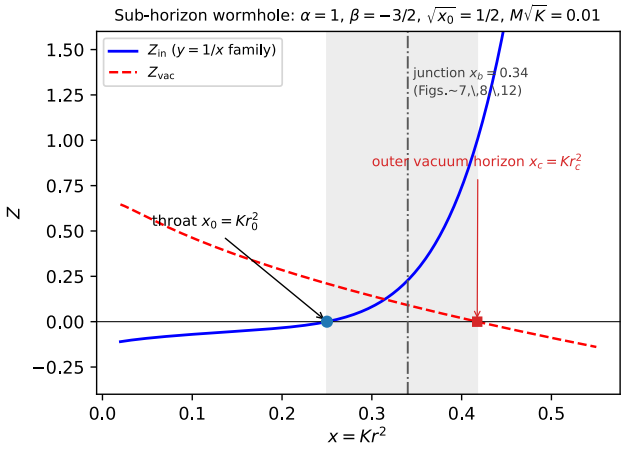


Fig. 5. (color online) The subhorizon family (29) (solid curves) and the exact vacuum $Z_{\rm vac}$ (dashed curve) are shown for $\alpha=1$, $\beta=-3/2$, $\sqrt{x_0}=1/2$, and $M\sqrt{K}=0.01$. The throat, $x_0=Kr_0^2$, lies inside the static patch; the shaded region indicates the junction window, bounded by the outer vacuum horizon $x_c=Kr_c^2$. The dash-dotted line marks the representative junction $x_b=0.34$ used in Figs. 8, 9, and 13.

The throat pressure (32) is seed-independent for the same reason; consequently, the window (31) and its lower edge $\sqrt{x_0}=\alpha/(2|\beta|)$ are properties of the theory rather than of any particular model. The dichotomy of Sec. IV is seed-independent in a slightly different sense: it is exhaustive. Every seed falls on one or the other side of the sign of $2x_0\dot{y}(x_0)+y(x_0)$ in (21), and there is no third possibility. Thus, no choice of y can yield a sub-horizon throat with non-decreasing redshift or a super-horizon one with a

CPC Accepted

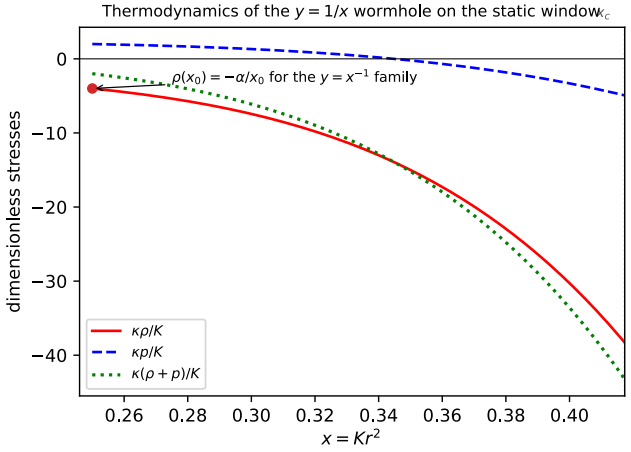


Fig. 6. (color online) Thermodynamics of the $y = 1/x$ wormhole, shown in the static window $x_0 \le x \le x_c$. The throat density is $-\alpha/x_0$, which is independent of the coupling within the $y = x^{-1}$ family, whereas the throat pressure is positive throughout the window (31).

static exterior. The conclusions regarding the throat location are fixed by the same identity, and the coupling bound that confines the excluded branch to $r_0 \gtrsim 50$ km is inherited from the compact-star analysis; hence, it is also independent of any choice of seed.

What the seed does control is the slope (21) and, through it, the throat density, the locations x_0 at which flare-out can be arranged, the profiles of ρ and p away from the throat, and the corresponding junction data and exotic budget. The tower (33) quantifies precisely this freedom within the sub-horizon branch: the throat density (34) takes both signs as s and w vary, while Fig. 4 shows the exoticity being traded between the density and pressure channels, with $\rho + p$ negative throughout. A different seed redistributes the exotic matter; it does not remove it.

This also resolves whether some seed might reproduce the behaviour attributed to Fig. 5 of Ref. [53]. It cannot, and the reason is structural rather than numerical. In that work, the shape function is prescribed and flare-out is examined afterwards; here, Z is solved for from the seed, and flare-out enters beforehand as the existence test (21), which a solution must pass before it is called a wormhole at all. A seed for which $\dot{Z}(x_0) < 0$ is not discarded as unphysical —it describes a maximal-area sphere, as at x_- in Sec. V—but neither is it identified as a throat. It is this type of accounting, rather than any difference in the theory, that distinguishes the two interpretations of the published numerical results.

VII. DARMOIS–ISRAEL COMPLETION AND THE EXOTIC BUDGET

The wormhole model assembled. The global construction can now be stated explicitly and is illustrated in Fig. 7. The interior potential is the exact isotropic solution (29) generated by the seed $y = 1/x$; the exterior is the vacuum (10). Proceeding outward from the throat, the final spacetime consists of three components: the *interior fluid region* $x_0 \le x \le x_b$, where Z is the physical potential and $\dot{Z} > 0$; the *thin matching shell* at $x = x_b$, where the interior is joined to the vacuum and the discontinuity in the extrinsic curvature is supported by the surface stresses $(\sigma, \mathcal{P})$ computed below; and the *vacuum envelope* $x_b \le x \le x_c$, where $Z_{\rm vac}$ is the physical potential. No region beyond x_c is included, because the $t = \text{const}$ slice ceases to be spacelike there; extension through that horizon is a separate question. The construction is then doubled across the throat, in the usual Morris–Thorne

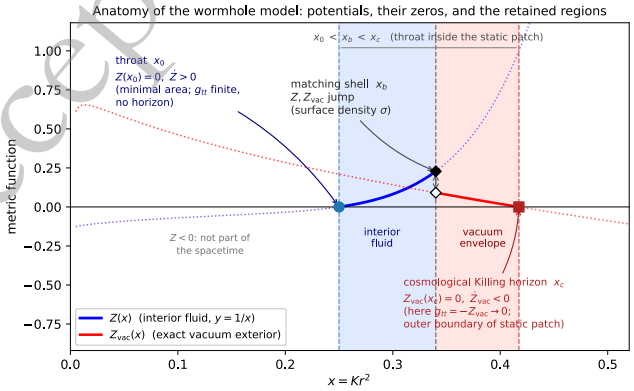


Fig. 7. (color online) How the wormhole model fits together. The interior potential $Z(x)$ (blue, solid only on the interior fluid interval $x_0 \le x \le x_b$) and the exact vacuum potential $Z_{\rm vac}(x)$ (red, solid only on the vacuum interval $x_b \le x \le x_c$) are shown as functions of $x = Kr^2$. Each potential is physical on only one side of the shell; the dotted continuations are unphysical extrapolations and are retained in neither the geometry nor the field equations. In particular, Z and $Z_{\rm vac}$ are never simultaneously active: the vacuum envelope is governed by $Z_{\rm vac}$ alone, and the dotted blue curve there is merely an extrapolation. The final spacetime consists of the interior fluid region $x_0 \le x \le x_b$ (blue band) joined at the thin shell x_b to the vacuum envelope $x_b \le x \le x_c$ (red band). The three loci are geometrically distinct: the throat x_0 is a simple zero of Z with $\dot{Z}(x_0) > 0$, corresponding to a minimal-area bridge; the matching surface x_b is *not* a zero of either potential but the radius at which Z and $Z_{\rm vac}$ are junction-matched, carrying the surface density σ (the double arrow marks the jump); and the cosmological Killing horizon x_c is a simple zero of $Z_{\rm vac}$ with $\dot{Z}_{\rm vac}(x_c) < 0$, forming the outer boundary of the static patch. The two zeros differ in kind: at the throat, the zero is in the spatial potential, so $g_{rr} = 1/Z$ diverges while $g_{tt} = -e^{2\nu}$ remains finite—a minimal-area bridge, not a horizon. By contrast, at x_c the static vacuum has $g_{tt} = -Z_{\rm vac}$, so its zero is a genuine Killing horizon at which ∂_t becomes null. The ordering $x_0 < x_b < x_c$ places the throat strictly inside the static patch. The interval $x < x_0$, where $Z < 0$, is not part of the spacetime.

CPC Accepted

fashion, to give the two sheets of the bridge. For the representative configuration ($\alpha = 1$, $\beta = -3/2$, $\sqrt{x_0} = 1/2$, $M\sqrt{K} = 0.01$), the ordering (11) gives $x_0 = 0.25 < x_b = 0.34 < x_c = 0.417$ in model units, or $r_0 = 0.50 < r_b = 0.58 < r_c = 0.65$.

Because $\rho + p = -(2\dot{Z} + 4Z/x)K/\kappa$ for the family (29) remains negative throughout its domain, the configuration must be terminated at a finite junction radius x_b within the static patch and matched to the vacuum solution $Z_{\rm vac}(x) = \alpha + \beta\sqrt{x} - 2M\sqrt{K}/\sqrt{x}$. Continuity of the induced metric is ensured by the usual proper-time normalisation on the shell Σ at areal radius $a = \sqrt{x_b/K}$, and the Lanczos equations yield the surface density and surface pressure

$$\sigma = -\frac{1}{4\pi a}\left(\sqrt{Z_{\rm vac}} - \sqrt{Z_{\rm in}}\right)\Big|_a , \tag{35}$$

$$\mathcal{P} = \frac{1}{8\pi}\left[\frac{\sqrt{Z_{\rm vac}} - \sqrt{Z_{\rm in}}}{a} + \frac{Z'_{\rm vac}}{2\sqrt{Z_{\rm vac}}} + \frac{2}{a}\sqrt{Z_{\rm in}}\right]_a , \tag{36}$$

where the prime denotes d/dr, and the final term in (36) is the interior extrinsic curvature $K^{\tau}{}_{\tau}$ generated by the steep redshift $e^{\nu} \propto r^{-2}$. Figure 10 shows the stresses across the junction window for the representative case. The surface density changes sign at $x_b \simeq 0.314$, so junctions in the outer part of the window carry *positive* surface energy, while the shell's own NEC combination $\sigma + \mathcal{P}$ remains mildly negative throughout. We emphasise that this surface NEC violation is a property of the particular junction chosen, not a consequence of the transparency theorem. The theorem constrains the matter at the throat and places no restriction on outer matching shells.

The static-patch completion admits the traditional wormhole portrait. Because $Z_{\rm in} < 1$ on the interior domain and $Z_{\rm vac} = \alpha + \beta\sqrt{x} - 2M\sqrt{K}/\sqrt{x} < 1$ throughout the static patch (for $\alpha = 1$, $\beta < 0$, $M > 0$), the composite geometry embeds isometrically in Euclidean 3-space over the entire static slice. Moreover, both ends of the embedding are governed by the same local behaviour. Near a simple zero of Z, the profile obeys $(dz/dr)^2 = (1 - Z)/Z$. Thus, at the throat, $z - z_0 \simeq \pm 2\sqrt{(r - r_0)/Z'_0}$, giving a vertical tangent at *finite* height; similarly, at the outer horizon, $z_c - z \simeq 2\sqrt{(r_c - r)/|Z'_c|}$, with the proper distance $\ell_c - \ell \simeq 2\sqrt{(r_c - r)/|Z'_c|}$ also finite. Figures 8 and 9 show the familiar flaring funnel, both in profile and as the traditional surface of revolution, with a mild kink at the shell where the extrinsic curvature jumps and a rim that *terminates at a vertical tangent on the cylinder* $r = r_c$ — the boundary of the static spatial slice — rather than flattening onto an asymptotic plane. The correct analogy is the

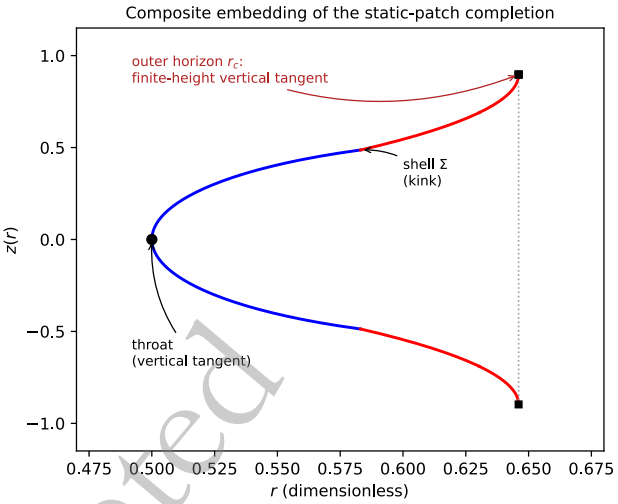


Fig. 8. (color online) Composite embedding for the static-patch completion: the interior $y = 1/x$ solution (blue) is joined across the shell Σ to the exact vacuum (red). The profile exhibits a vertical tangent at the wormhole throat, a finite kink at the shell, and a second vertical tangent at the outer vacuum horizon r_c, which is reached at finite embedding height and finite proper distance.

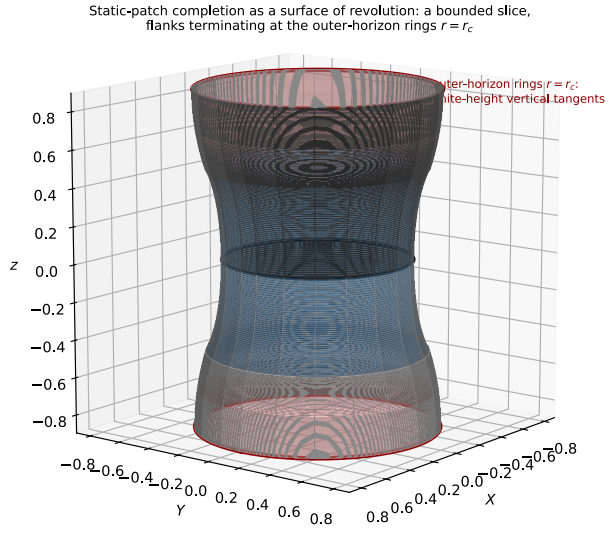


Fig. 9. (color online) The same composite geometry represented as a surface of revolution: a traditional hourglass, with the throat ring at the waist, dashed shell rings where the interior (blue) meets the vacuum (red), and two bold rings of radius r_c at which the flanks terminate with vertical tangents at the outer vacuum horizon. The slice is bounded: it neither opens onto flat planes nor continues as an infinite tube. The axes are equally scaled.

static slice of de Sitter space, whose embedding is a hemisphere meeting its equator vertically, not an infinite cylinder. The wormhole flares out normally at its throat, and the second vertical tangent is caused by the outer Killing horizon of the Vegh vacuum, not by any failure of

CPC Accepted

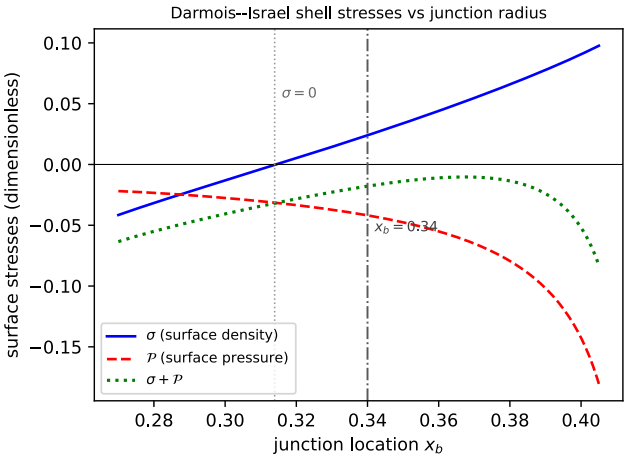


Fig. 10. (color online) Darmois–Israel surface stresses of the completing shell as a function of the junction location; the dot-dashed line indicates the representative junction at $x_b = 0.34$. The surface density is positive for $x_b \gtrsim 0.314$, whereas, for the representative configuration, the combination $\sigma + \mathcal{P}$ remains negative throughout the displayed interval—a property of this particular completion, not a requirement of the transparency theorem.

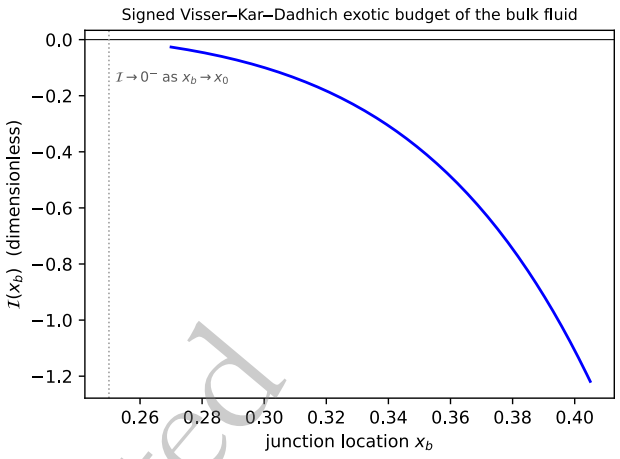


Fig. 11. (color online) The signed Visser–Kar–Dadhich exotic budget (37) is evaluated for the bulk fluid across the junction window. It remains negative throughout, with $\mathcal{I}(x_b) \to 0^-$ as $x_b \to x_0$; thus, its magnitude can be made arbitrarily small by moving the junction toward the throat.

flare-out. The $t = \text{const}$ slice simply ceases to be spatial beyond r_c; extension of the spacetime through the horizon is a separate question not addressed here.

The exotic matter content of the bulk fluid is finite and can be expressed explicitly. Evaluating the Visser–Kar–Dadhich measure on the bounded domain $[x_0, x_b]$ yields, in closed form,

$$\begin{aligned}\mathcal{I}(x_b) &\equiv \int_{x_0}^{x_b} (\rho + p)\, 4\pi r^2\, dr \\ &= -\frac{4\pi K^{-1/2}}{455\,\kappa\, x_0^7}\Big(182\,\alpha\, x_0^{15/2} - 260\,\alpha\, x_0^7\sqrt{x_b} \\ &\quad + 78\,\alpha\, x_b^{15/2} + 84\beta\sqrt{x_0}\, x_b^{15/2} \\ &\quad + 91\beta\, x_0^8 - 175\beta\, x_0^7 x_b\Big), \end{aligned} \tag{37}$$

verified against direct quadrature to machine precision, and shown in Fig. 11. The budget vanishes as $x_b \to x_0$, and its magnitude increases monotonically across the window. As in general relativity, the exotic bulk content can be made arbitrarily small by moving the junction toward the throat [9]. In the present model, the surface stresses shown in Fig. 10 remain finite in that limit — here realised in exact closed form within massive gravity.

A. Linearised stability of the shell

The radial dynamics of the shell follow by promoting the junction radius to $a = a(\tau)$. The angular component of the extrinsic curvature is then $K^\theta{}_\theta = \sqrt{Z + \dot{a}^2}/a$ on each side of the shell, and the Lanczos constraint can be rearranged into the standard energy equation $\dot{a}^2 + V(a) = 0$, with

$$V(a) = Z_{\rm in} - \left[\frac{u}{2} + \frac{Z_{\rm in} - Z_{\rm vac}}{2u}\right]^2, \qquad u \equiv 4\pi a\,\sigma(a), \tag{38}$$

The system is closed by a barotropic surface equation of state with response $\eta = d\mathcal{P}/d\sigma$ and the test-shell conservation law $\sigma' = -(2/a)(\sigma + \mathcal{P})$. At this initial stage, we neglect the flux correction sourced by the interior fluid and defer its exact treatment. Static solutions are stable if and only if $V''(a_0) > 0$. Evaluating $V''(a_0)$ across the positive-density branch of the representative configuration, Fig. 12, we find that it depends only weakly on η and vanishes only near $\eta \simeq -3\times10^2$ to -5×10^2, depending on the junction location. Stabilisation would therefore require a surface response far outside any physically plausible range. The zero-flux test-shell closure thus yields radial instability for the completing shells of the $y = 1/x$ configuration. Because the interior fluid has $\rho + p \neq 0$ at the junction, a moving shell generates a nonvanishing momentum-flux term, and a definitive physical conclusion requires its restoration. As a diagnostic, however, the result is consistent with the generic fragility of thin-shell wormholes [59]. Shells matched to a vacuum that possesses a cosmological zero are known to be similarly delicate in general relativity [60], so the behaviour found here is not peculiar to the mass term. Moreover, the seed tower (33) now allows this issue to be scanned systematically: whether steeper seeds, or junctions drawn closer to the throat where the bulk budget shrinks, admit stable shells is a sharply posed question that we leave to the systematic sweep.

CPC Accepted

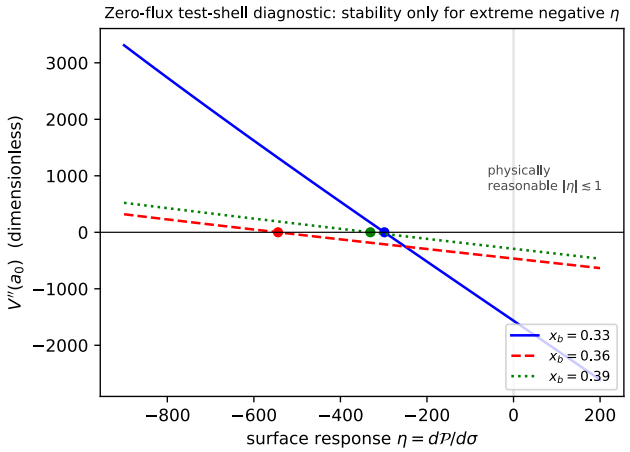


Fig. 12. (color online) Zero-flux test-shell diagnostic: the discriminant $V''(a_0)$ is shown as a function of the surface response $\eta = d\mathcal{P}/d\sigma$ for three junction locations, $x_b = Ka_0^2$ (model units with $K = 1$). Zero crossings (dots) occur only near $\eta \simeq -3\times10^2$ to -5×10^2, far outside the physically plausible range $|\eta| \lesssim 1$ (shaded). Thus, all such junctions are radially unstable within this closure.

VIII. LIGHT BENDING IN THE STATIC-PATCH COMPLETION

Light bending has already been calculated for black holes in this theory, both for particle orbits and lensing in the dRGT background [61] and for the effect of the graviton mass on the deflection angle [62]. The wormhole case differs in one key respect that governs the entire calculation: the exterior is not asymptotically flat. The complete configuration — interior, shell, and vacuum — provides a well-defined lensing target, and the non-flat asymptotics determines the appropriate observable. The deflection must be defined with respect to emission and reception at finite radii inside the static patch, rather than at infinity. For a photon with impact parameter $b = r_{\rm min}/\sqrt{A(r_{\rm min})}$, where $A = e^{2\nu}$ is the (continuous) temporal potential of the composite metric — written A here to avoid collision with the fiducial profile $F(r)$ of Sec. III — and $H = Z$ is its (discontinuous) radial potential, the azimuthal sweep from the turning point to an observer at $R_{\rm obs}$ is

$$\Delta\phi(b) = 2\int_{r_{\rm min}}^{R_{\rm obs}} \frac{dr}{r^2\sqrt{H(r)\left[b^{-2}A(r)^{-1} - r^{-2}\right]}}, \qquad (39)$$

We quote the *finite-radius excess azimuth* $\hat{\alpha}(b) = \Delta\phi - 2\arccos(r_{\rm min}/R_{\rm obs})$ relative to the Euclidean chord between the same radii. This quantity reduces to the standard deflection $\Delta\phi - \pi$ when $R_{\rm obs} \to \infty$ in an asymptotically flat spacetime. In the present non-asymptotically-flat setting, $\hat{\alpha}$ is a coordinate diagnostic rather than an invariant deflection angle. The tetrad-based finite-distance observable, which supplements (39) with the local incidence angles at the source and receiver, is deferred.

Figure 13 shows $\hat{\alpha}(b)$ for the representative configuration with $R_{\rm obs} = 0.97\,r_c$. Rays with turning points in the vacuum probe the exterior $\alpha + \gamma r/2 - 2M/r$. As the turning point crosses the shell, the deflection curve remains continuous but its slope changes, providing a lensing signature of the surface layer. As b decreases toward the throat value, the excess azimuth grows without bound. This divergence signals an unstable circular photon orbit at the throat, as can be shown without appealing to $H \to 0$. On the reflection-symmetric doubled wormhole, the photon motion is governed by $\mathcal{B} = r^2/A$ along the proper radial distance ℓ. Symmetry requires $d\mathcal{B}/d\ell = 0$ at the throat. For the present seed, $A \propto r^{-4}$ gives $\mathcal{B} \propto r^6$, and the flare-out property $d^2r/d\ell^2 > 0$ makes the throat a minimum of $\mathcal{B}$ — equivalently, a maximum of the photon potential A/r^2 — and hence an unstable circular light orbit with the associated logarithmic strong-deflection divergence. The inset of Fig. 13 confirms this numerically: the excess azimuth is linear in $-\ln(b/b_{\rm th} - 1)$ with slope $\simeq 1.15$ as $b \to b_{\rm th}^+$. This check is nontrivial: reflection-symmetric throats can support either stable or unstable light rings, depending on the metric. A full strong-deflection-limit expansion of (39), and the image structure it implies — with the caveat that a traversable throat transmits photons between the two universes, so any shadow depends on the illumination of both sides — are natural continuations.

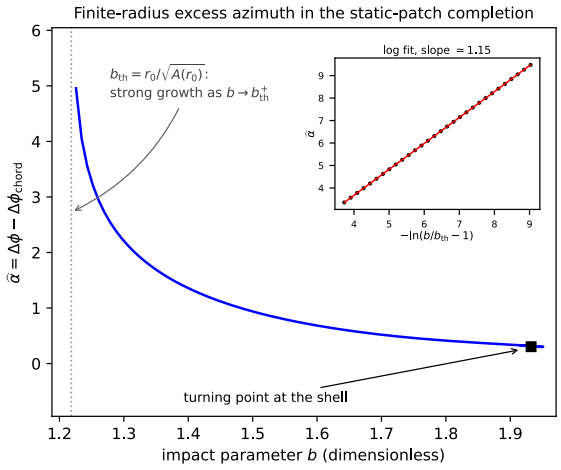


Fig. 13. Finite-radius excess in azimuthal angle $\Delta\phi - \Delta\phi_{\rm chord}$ for light rays through the static-patch completion, for an observer at $R_{\rm obs} = 0.97\,r_c$. The squares mark turning points at the shell; the dotted line indicates the throat impact parameter $b_{\rm th} = r_0/\sqrt{F(r_0)}$, as this value is approached, the excess increases rapidly. Inset: the same data plotted against $-\ln(b/b_{\rm th} - 1)$; the linearity (slope $\simeq 1.15$) confirms the logarithmic law expected for an unstable circular light orbit.

CPC Accepted

IX. DISCUSSION AND OUTLOOK

The results form a coherent picture. In Vegh–dRGT massive gravity, the graviton sector does not affect the radial null energy condition and therefore cannot replace the exotic matter required by a Morris–Thorne throat. Moreover, under the effective-stress decompositions used in previous studies, claims to the contrary are incompatible with the flare-out identity. Instead, the graviton sector constrains *where* throats may exist and *how* they are dressed. Isotropic wormholes with non-decreasing redshift are forced beyond the cosmological zero of the theory's own vacuum and, through the compact-star bound of the companion paper, beyond fifty kilometres. Astrophysical throats that admit a static Vegh-vacuum exterior are instead confined to the steep-redshift branch. For this branch, we have exhibited an exact family with a universal, coupling-independent throat density and a graviton-generated window of positive throat pressure, completed by a thin shell whose stresses and exotic budget are known in closed form.

Several extensions naturally follow. The seed tower (33) explicitly maps the isotropic sub-horizon space, and its phase diagram shows how the throat exchanges exoticity between the density and pressure channels around the universal landmark $w = 1/2$. Extending the linearised shell analysis across the tower, with the interior flux term restored, will determine whether stable completions exist. The anisotropic sector with the shape function derived rather than imposed, the strong-deflection expansion of (39) with its image ladder and transmission-dependent shadow structure, and the throat perturbation problem all remain within reach of the present formalism. Finally, the interplay established here between compact-star constraints and wormhole existence—with the same coupling window governing both—suggests that multimessenger bounds on the graviton mass translate, in this theory, into exclusion statements about entire classes of exotic compact objects. This direction will be pursued in future work.

DECLARATION OF COMPETING INTEREST

The authors declare that they have no financial or personal relationships that could have influenced the research presented in this paper.

DATA AVAILABILITY

The data supporting the findings of this study are available from the corresponding author upon reasonable request. All numerical results reported in this work were obtained using the theoretical framework and equations described in the manuscript.

CPC Accepted

References

[1] A. Einstein and N. Rosen, Phys. Rev. **48**, 73 (1935)
[2] C. W. Misner and J. A. Wheeler, Ann. Phys. **2**, 525 (1957)
[3] M. S. Morris and K. S. Thorne, Am. J. Phys. **56**, 395 (1988)
[4] M. S. Morris, K. S. Thorne, and U. Yurtsever, Phys. Rev. Lett. **61**, 1446 (1988)
[5] M. Visser, Phys. Rev. D **39**, 3182 (1989)
[6] M. Visser, *Lorentzian Wormholes. From Einstein to Hawking* (American Institute of Physics, Woodbury, New York, 1995).
[7] D. Hochberg and M. Visser, Phys. Rev. D **56**, 4745 (1997), arXiv: gr-qc/9704082
[8] F. S. N. Lobo, in *Wormholes, Warp Drives and Energy Conditions*, Vol. 189, edited by F. S. N. Lobo (Springer International Publishing, Cham, 2017) pp. 11–34.
[9] M. Visser, S. Kar, and N. Dadhich, Phys. Rev. Lett. **90**, 201102 (2003)
[10] K. K. Nandi, Y.-Z. Zhang, and K. B. V. Kumar, Phys. Rev. D **70**, 127503 (2004)
[11] M. Visser, Nucl. Phys. B **328**, 203 (1989)
[12] G. A. S. Dias and J. P. S. Lemos, Phys. Rev. D **82**, 084023 (2010)
[13] S. Sushkov, Phys. Rev. D **71**, 043520 (2005)
[14] F. S. N. Lobo, Phys. Rev. D **71**, 084011 (2005)
[15] F. S. N. Lobo, Phys. Rev. D **71**, 124022 (2005)
[16] F. S. N. Lobo, Phys. Rev. D **73**, 064028 (2006)
[17] P. K. F. Kuhfittig, Gen. Relativ. Gravit. **41**, 1485 (2009)
[18] J. A. González, F. S. Guzmán, N. Montelongo-García, and T. Zannias, Phys. Rev. D **79**, 064027 (2009)
[19] T. Harko, F. S. N. Lobo, S. Nojiri, and S. D. Odintsov, Phys. Rev. D **84**, 024020 (2011)
[20] M. Zubair, S. Waheed, and Y. Ahmad, Eur. Phys. J. C **76**, 444 (2016)
[21] P. H. R. S. Moraes and P. K. Sahoo, Phys. Rev. D **96**, 044038 (2017)
[22] E. Elizalde and M. Khurshudyan, Phys. Rev. D **98**, 123525 (2018)
[23] P. K. Sahoo, P. H. R. S. Moraes, P. Sahoo, and G. Ribeiro, Int. J. Mod. Phys. D **27**, 1950004 (2018), arXiv: 1802.02465[gr-qc]
[24] E. Elizalde and M. Khurshudyan, Phys. Rev. D **99**, 024051 (2019)
[25] N. Godani and G. C. Samanta, Chin. J. Phys. **62**, 161 (2019)
[26] P. H. R. S. Moraes, W. De Paula, and R. A. C. Correa, Int. J. Mod. Phys. D **28**, 1950098 (2019)
[27] A. Banerjee, K. N. Singh, M. Jasim, and F. Rahaman, Ann. Phys. **422**, 168295 (2020)
[28] A. K. Mishra, U. K. Sharma, V. C. Dubey, and A. Pradhan, Astrophys. Space Sci. **365**, 34 (2020)
[29] A. Chanda, S. Dey, and B. C. Paul, Gen. Relativ. Gravit. **53**, 78 (2021)
[30] S. Rastgoo and F. Parsaei, Nucl. Phys. B **1011**, 116797 (2025)
[31] M. Zubair, R. Saleem, Y. Ahmad, and G. Abbas, Int. J. Geom. Methods Mod. Phys. **16**, 1950046 (2019)
[32] J. Luís Rosa and P. M. Kull, Eur. Phys. J. C **82**, 1154 (2022)
[33] J. L. Rosa, Phys. Rev. D **103**, 104069 (2021)
[34] H. Moradpour, N. Sadeghnezhad, and S. Hendi, Can. J.

Phys. **95**, 1257 (2017)
[35] S. Halder, S. Bhattacharya, and S. Chakraborty, Mod. Phys. Lett. A **34**, 1950095 (2019)
[36] G. Mustafa, M. R. Shahzad, G. Abbas, and T. Xia, Mod. Phys. Lett. A **35**, 2050035 (2020)
[37] G. Mustafa, S. Waheed, M. Zubair, and T.-C. Xia, Chin. J. Phys. **65**, 163 (2020)
[38] C. de Rham and G. Gabadadze, Phys. Rev. D **82**, 044020 (2010), arXiv: 1007.0443[hep-th]
[39] C. de Rham, G. Gabadadze, and A. J. Tolley, Phys. Rev. Lett. **106**, 231101 (2011), arXiv: 1011.1232[hep-th]
[40] S. F. Hassan and R. A. Rosen, Phys. Rev. Lett. **108**, 041101 (2012), arXiv: 1106.3344[hep-th]
[41] K. Hinterbichler, Rev. Mod. Phys. **84**, 671 (2012), arXiv: 1105.3735[hep-th]
[42] C. de Rham, Living Rev. Relativ. **17**, 7 (2014), arXiv: 1401.4173[hep-th]
[43] D. Vegh, Holography without translational symmetry (2013), arXiv: 1301.0537 [hep-th].
[44] R. A. Davison, Phys. Rev. D **88**, 086003 (2013), arXiv: 1306.5792[hep-th]
[45] M. Blake, D. Tong, and D. Vegh, Phys. Rev. Lett. **112**, 071602 (2014), arXiv: 1310.3832[hep-th]
[46] R.-G. Cai, Y.-P. Hu, Q.-Y. Pan, and Y.-L. Zhang, Phys. Rev. D **91**, 024032 (2015), arXiv: 1409.2369[hep-th]
[47] S. G. Ghosh, L. Tannukij, and P. Wongjun, Eur. Phys. J. C **76**, 119 (2016), arXiv: 1506.07119[gr-qc]
[48] T. Katsuragawa, S. Nojiri, S. D. Odintsov, and M. Yamazaki, Phys. Rev. D **93**, 124013 (2016), arXiv: 1512.00660[gr-qc]
[49] S. H. Hendi, G. H. Bordbar, B. E. Panah, and S. Panahiyan, J. Cosmol. Astropart. Phys. (07), 004 (2017), arXiv: 1701.01039[gr-qc]
[50] B. E. Panah and H. L. Liu, Phys. Rev. D **99**, 104074 (2019), arXiv: 1805.10650[gr-qc]
[51] T. Tangphati, A. Chatrabhuti, D. Samart, and P. Channuie, Phys. Rev. D **102**, 084026 (2020), arXiv: 2003.01544[gr-qc]
[52] N. Kamma, P. Wongjun, R. Nakarachinda, and B. Gumjudpai, J. Phys. Conf. Ser. **1719**, 012018 (2021)
[53] A. Dutta, D. Roy, N. J. Pullisseri, and S. Chakraborty, Eur. Phys. J. C **83**, 500 (2023), arXiv: 2306.06911[gr-qc]
[54] P. Bhar, Eur. Phys. J. C **85**, 3 (2025), arXiv: 2408.02717[gr-qc]
[55] J. Kumar, S. K. Maurya, and S. Kiroriwal, Eur. Phys. J. C **84**, 1305 (2024)
[56] S. Chaudhary, S. Maurya, and J. Kumar, Phys. Dark Universe **49**, 102019 (2025)
[57] A. Dutta, D. Roy, and S. Chakraborty, Int. J. Mod. Phys. A **40**, 2450135 (2025), arXiv: 2410.04533[gr-qc]
[58] A. Landry, Y. Sekhmani, S. K. Maurya, A. Ali, and E. N. Saridakis, Int. J. Geom. Methods Mod. Phys. **23**, 2650192 (2026), arXiv: 2508.06290[gr-qc]
[59] E. Poisson and M. Visser, Phys. Rev. D **52**, 7318 (1995), arXiv: gr-qc/9506083
[60] F. S. N. Lobo and P. Crawford, Class. Quantum Grav. **21**, 391 (2004)
[61] S. Panpanich, S. Ponglertsakul, and L. Tannukij, Phys. Rev. D **100**, 044031 (2019), arXiv: 1904.02915[gr-qc]
[62] H. Abdusattar, Y.-X. Han, A. Rusul, and S.-B. Kong, Eur. Phys. J. C **86**, 141 (2026), arXiv: 2505.03386[gr-qc]

CPC Accepted